Alterations in spontaneous delta and gamma activity might provide clues to detect changes induced by amyloid-β administration

EJN European Journal of Neuroscience FENS Federation of European Neuroscience Societies

Alterations in spontaneous delta- and gamma-activity might provide clues to detect changes induced by amyloid-β administration

Journal:	*European Journal of Neuroscience*
Manuscript ID	EJN-2017-08-24889.R2
Manuscript Type:	Research Report
Date Submitted by the Author:	n/a
Complete List of Authors:	Hidisoglu, Enis; Akdeniz University, Biophysics Kantar Gok, Deniz; Akdeniz University, Biophsics Er, Hakan; Akdeniz University, Biophysics Acun, Alev; Akdeniz Universitesi, Biophysics Yargicoglu, Piraye; Akdeniz University, Biophysics
Key Words:	Alzheimer's disease, amyloid-β peptide, electroencephalography, brain oscillations, rat

Authors' Responses to Reviewers

We thank the reviewer for re-evaluating of the paper and helpful comments. We answered the reviewer's question, and related section was improved. So, we hope that the responses have the potential to match these questions satisfactorily.

Sincerely

Piraye Yargicoglu, PhD

Corresponding Author

Reviewer #1:

We thank you for your valuable opinion.

Reviewer #2:

We thank you for your valuable opinion.

Reviewer #3:

The authors adequately answered some of the concerns raised by the reviewers. However, there is still some point that clearly needs clarification before publication. From the new figure 3, which was definitively needed, it is clear that the authors do not know when they are analyzing the data. Indeed, the height 2 Hz peak with the absence of theta peak in the power spectrum clearly indicates that the authors mainly record either SWS or LIA, an awake state devoid of theta oscillations. However, without EMG electrodes and/or video recording of the rat, it is impossible to say. This actually changes the output of the study (sleep vs awake alterations). In conclusion, I believe that the amount of data analyzed in this study (160 sec of data in an undetermined brain state) do not support the strong conclusion state by the authors. I really like the study but I would recommend performing recording during at least 2 to 4 hours and looking at the EEG changes depending on the brain state of the animal (wake vs SWS vs REM sleep).

Response

- We thank the reviewer for these critical comments. In this study, we recorded spontaneous EEG activity in the freely moving rats without anesthesia by using chronic electrode implantation to eliminate effects of anesthesia or sleep. During the recording sessions, EEG activity and rats' behavior were examined visually by the experimenter. The experimenter did not observe any specific changes indicating that the rats were at slow-wave sleep (SWS) or rapid-eye-movement (REM) sleep, even if video recording was not taken during the EEG recording. As the reviewer stated, it would be more useful to determine sleep/wake cycle by recording EEG and EMG activity. But, sleep can also be defined by rats' behavior such as absence of movement as well as slow waves observed in EEG activity. As you know, if we want to determine the stages of sleep, we can more precisely distinguish SWS and REM sleep, which are two well-characterized physiological states in rats, by taking advantage of the EEG and EMG activity. Also, we know that SWS can typically not be recorded during laboratory recordings unless there has been substantial sleep deprivation preceding the study in both human and animals. On the other hand, you are right, large irregular activity (LIA) has a predominantly lower oscillation frequency but contains some sharp spikes (We did not observe any sharp waves in EEG activity during recording.). Considering these knowledge and our observations during recording session, it is therefore possible to say that we have recorded the EEG activity in the awake state of the rats. Following sentence was added to the Materials and Methods Section; "EEG recordings were obtained via chronically implanted electrodes from freely moving rats to eliminate possible effects of anesthesia on brain activity."

- You are right that 160 sec is so short time to determine brain state. But, we did not record 160 sec-EEG activity. In total, EEG recording was lasted 20 minutes (1200 sec) for

each rat. Since, it has been provided to adaptation of freely moving rats to the sound-attenuated recording environment in the first 10 minutes, we did not use this first 10 min for further analysis. The last 10-minute EEG recording was used for frequency analysis. The 10-minute EEG data were processed in 2000 ms long epochs (300 epochs) and, the epochs contaminated by movement artifacts were eliminated manually. In conclusion, we used 80 epochs (2 sec long), which were free of movement artifacts, to determine changes in EEG activity for each rat. We think that these epoch numbers and duration are sufficient to evaluate the brain state of animal. Also, there are many studies in the literature that we can be referring to our time window using for analysis (Adler *et al.*, 2003; Wang *et al.*, 2016; Hernandez-Gonzalez *et al.*, 2017; Taylor *et al.*, 2017) .

On the other hand, we believe that detecting of changes in EEG activity depending on brain functional state by performing recording during 2 to 4 hours or maybe longer, it will provide more comprehensive and valuable information. In future studies, you can be sure that we will consider your valuable comment. We thank you so much again.

References

Adler, G., Brassen, S. & Jajcevic, A. (2003) EEG coherence in Alzheimer's dementia. *J Neural Transm*, **110**, 1051-1058.

Hernandez-Gonzalez, M., Hernandez-Arteaga, E., Guevara, M.A., Almanza-Sepulveda, M.L., Ramirez-Renteria, M.L., Arteaga-Silva, M. & Bonilla-Jaime, H. (2017) Prenatal stress suppresses the prefrontal and amygdaline EEG changes associated with a sexually-motivated state in male rats. *Physiol Behav*, **182**, 86-92.

Taylor, J.A., Rodgers, K.M., Bercum, F.M., Booth, C.J., Dudek, F.E. & Barth, D.S. (2017) Voluntary Control of Epileptiform Spike-Wave Discharges in Awake Rats. *J Neurosci*, **37**, 5861-5869.

Wang, J., Wang, J., Xing, G.G., Li, X.L. & Wan, Y. (2016) Enhanced Gamma Oscillatory Activity in Rats with Chronic Inflammatory Pain. *Front Neurosci-Switz*, **10**.

Title: Alterations in spontaneous delta- and gamma-activity might provide clues to detect changes induced by amyloid-β administration

Enis Hidisoglu, Deniz Kantar-Gok, Hakan Er, Alev Duygu Acun, Piraye Yargicoglu*

Akdeniz University Faculty of Medicine Department of Biophysics, Antalya, TURKEY

Running Title: Amyloid-β–induced significant changes in brain oscillations

Word count: 7945

***Corresponding Author:** Piraye Yargicoglu

Akdeniz University Faculty of Medicine

Department of Biophysics, Antalya/TURKEY.

Phone: Work: 0 090-242-2496906

Fax: 0 090-242-2274495

E-Mail: pakkiraz@akdeniz.edu.tr

Abstract

Alzheimer's disease (AD) is the most prevalent form of dementia and has an increasing incidence. The neuropathogenesis of AD is suggested to be a result of the accumulation of amyloid-β (Aβ) peptides in the brain. To date, Aβ-induced cognitive and neurophysiologic impairments have not been illuminated sufficiently. Therefore, we aimed to examine how spontaneous brain activities of rats changed by injection of increasing Aβ doses into the brain hemispheres, and whether these changes could be used as a new biomarker for the early diagnosis of the AD. Rats were randomized into following groups; sham (Sham) and 7 Aβ-treated (i.c.v.) groups in increasing concentrations (from Aβ-1 to Aβ-7). After recovery, EEG recordings were obtained from implanted electrodes from eight electrode locations, and then spectral and statistical analyses were performed. A significant decrement in gamma activity was observed in all Aβ groups compared with the sham group. In delta activity, we observed significant changes from Aβ-4 to Aβ-7 group compared with sham and Aβ-1 groups. Delta coherence values were decreased from Aβ-4 to Aβ-7 and Aβ-5 to Aβ-7 groups for frontal and temporal electrode pairs, respectively. A gradual increment was observed in $A\beta_{1\text{-}42}$ level till Aβ-4 group. Positive correlation for global delta power and negative correlation for global gamma power between $A\beta_{1\text{-}42}$ peptide levels were detected. Consequently, it is conceivable to suggest gamma oscillation might be used to detect early stages of AD. Moreover, changes in delta activity provide information about the onset of major pathologic changes in the progress of AD.

Keywords: Alzheimer's disease, amyloid-β peptide, electroencephalography, brain oscillations, rat

Introduction

Alzheimer's disease (AD) is the most prevalent form of dementia worldwide and has an increasing incidence in modern societies. Memory deficits, behavioral changes, and cognitive decline are the most prominent features of the disease. AD is characterized histopathologically by the deposition of extracellular amyloid plaques and intracellular neurofibrillary tangles in the brain (Masliah *et al.*, 2001; Turner *et al.*, 2003). The hippocampus, limbic and associated cortices are the most important brain regions among the main targets of amyloid-β (Aβ) aggregates, which initiate pathologic processes in these regions and several other structures of the brain in patients with AD (Uylings & de Brabander, 2002). Therefore, the detection of possible changes caused by the accumulation of Aβ peptide in the early stage of AD is of special interest for scientists; it is important to detect AD early with more cost-efficient and easy-to-use methods, and it is essential for improving treatment management before permanent brain damage occurs.

Many studies related to AD have focused on biochemical mechanisms, including neurodegenerative processes initiated by the accumulation of Aβ peptide (Benilova *et al.*, 2012; Sheng *et al.*, 2012). These studies yielded considerable information describing some aspects of the disease, usually associated with the last stages. However, therapeutic approaches based on the results of these studies have either little or no benefit in changing the course of disease progression (Corbett & Ballard, 2012). Therefore, early detection of AD might be very beneficial to intervene earlier in the course of the disease. Nowadays, some biomarkers are available for the evaluation of AD (Dubois *et al.*, 2007; Jack *et al.*, 2010; Albert *et al.*, 2011; McKhann *et al.*, 2011; Sperling, 2011). These biomarkers include brain hypermetabolism as measured via fluorodeoxyglucose (FDG)-positron emission tomography (PET), brain amyloid load measured via ligand PET, and brain atrophy and abnormality mapping of structural brain connectivity as detected using magnetic resonance imaging

(MRI). However, these markers have some drawbacks: they are relatively expensive, invasive, have low temporal resolution, and impact patients due to the effects of radiation exposure. Accordingly, they cannot be used generally in all kinds of patients with AD. In contrast, electroencephalography (EEG) recordings obtained in different conditions represent an ideal low cost and noninvasive tool for clinical and experimental applications. EEG is also widely available and faster to use than other imaging methods such as MRI and PET (Bickford, 1976). EEG rhythms emerge as a consequence of the electrical activity of the brain, which is the summation of oscillations in different frequency bands, considered as the natural frequencies of neuronal networks, and are directly very relevant to cognition. It has been reported that these rhythms in various frequency bands reflect different stages of information processing and activate very large neural networks, even in the simplest cognitive functions. Human studies have indicated that EEG is a powerful method and might be used for the diagnosis of AD, as well as to identify abnormalities in cognitive processes at high temporal resolution in the disease (Babiloni *et al.*, 2007; Yener & Basar, 2010). For these reasons, cognitive deficits that occurred at the early stages of AD could be examined on the basis of the relevant neural network dysfunction (Palop & Mucke, 2010; Wesson *et al.*, 2011), which could be detected using EEG. We preferred to use EEG to detect early changes in AD according to the accumulation of $A\beta_{1\text{-}42}$ peptide because of these advantages and the information it provides.

In the literature, there are several transgenic and non-transgenic animal models of AD. Transgenic models have contributed significant insights into the pathophysiology of amyloid-β toxicity and lesions at the symptomatic level. Nevertheless, transgenic animal models have some drawbacks as compared with non-transgenic animal models, such as injection of aggregated $A\beta_{25\text{-}35}$, $A\beta_{1\text{-}40}$ or $A\beta_{1\text{-}42}$ into rat cerebral ventricles (Balducci & Forloni, 2011; Braidy *et al.*, 2012). First, the neuropathology that occurs in most transgenic animal models

does not fully replicate all aspects of human disease and stays very simple as compared with the complex neuropathology observed in humans. Secondly, making any comparison between transgenic animal models is also difficult because of the difference of genetic manipulations used in transgenic animal models. Finally, perhaps most importantly, transgenic animal models only relate to the familial early-onset form of AD, which is responsible for a very small percentage of Alzheimer's cases seen around the world (Lecanu & Papadopoulos, 2013). Researchers also try to focus on the etiology rather than the symptomatology of disease using a pharmacologic approach in non-transgenic animal models. There are various forms of Aβ peptide used to develop non-transgenic animal models, which display an amyloidogenic cascade and related amyloid peptide pathologic pathways. For this purpose, the most commonly used forms of Aβ peptide are $A\beta_{1-40}$ and $A\beta_{1-42}$, injected either as intracerebroventricular or intrahippocampal (Malin *et al.*, 2001; Lecanu *et al.*, 2006). These pharmacologic AD models have provided new opportunities to examine biochemical, cellular, and neurophysiologic mechanisms underlying AD pathology, and hence have an essential role in the investigation of the Aβ peptide contribution in AD pathogenesis. On the other hand, only a few EEG studies in the literature were conducted using non-transgenic animal models of AD (Wang *et al.*, 2002; Sanchez-Alavez *et al.*, 2007; Mugantseva & Podolski, 2009), and Aβ-induced cognitive and neurophysiologic impairments were not investigated sufficiently. The exact role of Aβ peptide accumulation in the disease progression is one of the central questions in AD research. To date, the effect of Aβ peptide injections into rat cerebral ventricles at increasing concentrations on brain oscillations has not been studied. We preferred to use the $A\beta_{1-42}$ peptide in this study because $A\beta_{1-42}$ is more hydrophobic and has a greater tendency to aggregate into fibrils and plaques compared to $A\beta_{1-40}$ (Jarrett *et al.*, 1993). Our aim was to evaluate the role of $A\beta_{1-42}$ peptide accumulation, which is significantly increased with certain forms of AD, on memory and EEG changes in awake rats. We also

aimed to determine whether the changes in brain electrical activity caused by accumulation of $A\beta_{1-42}$ peptide could be used for the detection of $A\beta_{1-42}$ peptide localization in the brain, and hence early detection of the disease.

Materials and methods

Animals

The rats were obtained from Akdeniz University Animal Care Unit. Ethical approval for this work was obtained from Akdeniz University Local Committee on Animal Research Ethics (ethics approval date and number: 09.11.2015/2015.01.11-3). All experimental protocols conducted on rats were performed in accordance with the standards established by the Institutional Animal Care and Use Committee at Akdeniz University. Male albino Wistar rats aged 3 months, weighing 250 to 300 g were housed in stainless steel cages and given food and water *ad libitium*. Animals were maintained at 12-h light-dark cycles and a constant temperature of 23±1°C at all times. All experimental protocols for all animals were performed at the same time interval (9:00 AM and 2:00 PM).

Animal Preparation

The rat model of AD was established as described previously (Li *et al.*, 2010; Gong *et al.*, 2011). $A\beta_{1\text{-}42}$ peptide (Sigma, USA) was injected into the lateral ventricles of the rats (5 µL per ventricle for each group). Stock solutions with different concentrations (1 µg/µL, 2 µg/µL, 3 µg/µL, 4 µg/µL, 6 µg/µL, 8 µg/µL, and 10 µg/µL) were prepared in sterile normal saline. To obtain the aggregated form of $A\beta_{1\text{-}42}$, the stock solutions were then incubated at 37°C for three days before use.

Surgery protocols

All rats had five days handling. Following handling sessions, the animals were randomly divided into eight groups (n=10 per group); 7 AD groups obtained by i.c.v. injection of $A\beta_{1\text{-}42}$ peptide in different concentrations and a sham group. Rats were anesthetized with a mixture of ketamine-based anesthetics (ketamine [50 mg/kg] and xylazine [10 mg/kg], intraperitoneally) and fixed on a stereotaxic instrument. During the anesthesia, the skull of the rats was placed in the stereotaxic apparatus and drilled for the implantation of

electrodes. Stainless steel screw electrodes were implanted bilaterally over the frontal (AP: 4.5 mm, ML: +2 and -2 mm), parietal (AP: -4.5 mm, ML: +3.5 and -3.5 mm), temporal (AP: -8.0 mm, ML: +6.6 and -6.6 mm) and occipital (AP: -8.0 mm, ML: +4.1 and -4.1 mm) regions, and the reference electrode was inserted into the cerebellum (AP: -12.72 mm, ML: 2.5 mm). All electrodes were embedded in dental acrylic and male pins were fixed to recording connectors. Following electrode implantation, either $A\beta_{1-42}$ peptide or saline (0.9% NaCl) was injected into the lateral ventricles (injected coordinates: AP: −0.8 mm, ML: −1.4 mm and +1.4 mm, DV: −4.0 mm) at 1 μL/minute using a Hamilton microsyringe. After administration of solutions and electrode implantation, at least 1 week (7 or 8 days) was allowed for recovery. During recovery, the rats were housed in individual cages with free access to food and water. After recovery, novel object recognition tests and EEG recordings were performed, respectively.

Novel object recognition test

The novel object recognition test was modified from a previously described method (Zhang *et al.*, 2012). The procedures are detailed schematically presented in Figure 1. The apparatus consists of a plexiglass box (80 cm x 80 cm x 80 cm), which is inside an evenly illuminated sound-proof room. We used a video camera to record the rats' behavior. The procedure includes 4 phases: pre-habituation, habituation, training, and testing. On the 1st day, the animals were brought to the testing room 30 min before the experiment to familiarize them with the environment. The rats were then allowed to freely explore the box in the absence of objects for 5 min. On the 2nd and 3rd day, rats were habituated to the empty box for 20 min per day. On the 4th day, each rat took a training trial followed by a testing trial. During the training trial, two identical objects were placed at two opposite positions within the box at the same distance from the nearest corner. The rats were allowed to explore the identical objects for 10 min, and then returned to their home cages. One hour later, the

animals were placed back in the same box, where one of the two familiar objects was switched to a novel one, to start a 5-min testing phase. All objects used in this study were different in shape but identical in size. They were fixed on the floor of the box to avoid movement. To preclude the existence of olfactory cues, the entire box and objects were always thoroughly cleaned with 70% ethanol after each trial.

Object exploration time was defined as the length of time when the animal directed its nose within 1 cm distance of the object, or sniffed or pawed the object. Sitting or standing on the object was not recognized as exploration. The exploration time was analyzed digitally using Noldus EthoVisionXT software (Noldus Information Technology, Leesburg, VA). The recognition index (RI) in the testing phase was calculated using the following formula:

$$\text{Recognition Index (RI)} = \frac{(T\ novel\ object\ )}{(T\ novel\ object + T\ familiar\ object)} \text{ x } 100\%$$

where T represents the exploring time of the object.

Recordings and analysis of EEG

All recordings were taken in a small box (40 x 40 x 40 cm) that had been placed in an electromagnetically shielded room in the morning, in a resting awake condition. EEG recording sessions lasted 20 minutes for each rat. The first 10 minutes of the recording sessions were adapted for freely moving rats in the sound-attenuated recording environment. The last 10-minute EEG recording was used for spectral analyses. The EEG was recorded bilaterally from frontal, parietal, temporal, and occipital locations. EEG recordings were obtained via chronically implanted electrodes from freely moving rats to eliminate possible effects of anesthesia on brain activity. All electrode impedances were less than 5 kOhm. The EEG signal was amplified (Brainamp EEG/EP Amplifier, Brain Products, Munich, Germany), band-pass filtered (0.1-300 Hz), and digitized at a 1000 Hz sampling rate (Brainvision Recorder, Brain Products, Munich, Germany). EEG analysis was conducted offline. The EEG data were processed in 2000-ms–long epochs; epochs contaminated by artifacts were

eliminated manually. For each group, approximately 80 artifact-free epochs were randomly selected and used for frequency analyses. Frequency analysis was performed using a Fast Fourier Transform (FFT) algorithm with Hanning window using the BrainVision Analyzer software (BrainProducts GmBH, Munchen). Eight electrode locations were used for the calculation of spectral EEG powers. The EEG variables chosen were absolute power in five frequency bands, delta (0.5-4 Hz), theta (4-8 Hz), alpha (8-13 Hz), beta (13-28 Hz), and gamma (28-48 Hz) (Bendat, 1982). Intra-hemispheric EEG coherences were calculated for the four electrode pairs FrA1-FrA2, PtA1-PtA2, TeA1-TeA2, and V1-V2, inter-hemispheric EEG coherences for the six electrode pairs FrA1-PtA1, FrA1-TeA1, PtA1-V1, Fr2-PtA2, FrA2-TeA2, and PtA2-V2 in each frequency band. Analyses were performed using the BrainVision Analyzer software (BrainProducts GmbH, Munchen).

Biochemical and immunohistochemical investigations

After making the electrophysiologic recordings, the rats were deeply anesthetized (20% urethane, 5 mL/kg, i.p.) and a cardiac cannula was placed. Brain tissues were perfused with heparinized isotonic (heparin (Innohep, Leo Pharma, Denmark), anticoagulant, and isotonic solution (0.9% NaCl) were administered via the cannula. Seven brains were immediately collected for enzyme-linked immunosorbent assay (ELISA) analysis. The isolated brain tissues were stored at -80°C until required for assay determinations. In addition, three brains were collected and fixed in 10% formaldehyde solution for immunohistochemical evaluations.

Measurement of $A\beta_{1-42}$ peptide levels

$A\beta_{1-42}$ levels in the supernatants of brain lysates were measured using a commercially available ELISA kit (SensoLyte Anti-Mouse/Rat b-amyloid (1-42) Quantitative ELISA *Colorimetric*, AnaSpec, Fremnot, CA, USA) in accordance with the manufacturer's instructions.

Paraffin embedding and immunohistochemistry

Brains were fixed in 10% formaldehyde and 5-µm–thick sections were collected onto superfrost ultra plus adhesion slides (Thermo Sci., Rockford, IL, USA). We stained randomly chosen slides from each group with cresyl violet for the assessment of the frontal, parietal, temporal, and occipital regions of the rat brain. The cresyl violet-stained slides were evaluated under a stereomicroscope (Zeiss Stemi SV 11, Oberkochen, Germany).

Immunoexpression of Aβ primary antibody (diluted 1:4000 in Labvision antibody diluent [Thermo, Fremont, CA, USA]) specific for Aβ peptide (Cell Signaling, Beverly, MA, USA) in all groups at four regions was obtained. Nonspecific binding was blocked with ultra V block (Labvision, Thermo, Fremont, CA, USA) and then incubated with biotinylated anti-rabbit secondary antibody (Vector Lab. Inc., Burlingame, CA, USA) at 1:400 dilution followed by a streptavidin-peroxidase complex (Labvision, Thermo, Fremont, CA, USA). Antibody-antigen complexes were visualized by incubation with 3,3'-Diaminobenzidine (DAB) (Dako, Carpinteria, CA, USA). Sections were examined using a bright-field microscope (Zeiss, Oberkochen, Germany). We additionally analyzed expression levels of the $A\beta_{1-42}$ peptide in all groups using the ImageJ (1.48v) software (NIH, USA), which confers semi-quantitative analysis of the staining percentage of the corresponding four regions in each group for $A\beta_{1-42}$ peptide immunoexpression, respectively.

Statistical analyses

All statistical analyses of the obtained data were performed using SPSS 18.0 (SPSS, Chicago, IL, USA) software for Windows. A repeated measure of ANOVA was used to determine the statistical significance of delta and gamma power over different locations and between the groups. During the analysis of spontaneous EEG, delta and gamma power

differences, repeated measures of ANOVA included the between-subjects factor as group (Aβ-1, Aβ-2, Aβ-3, Aβ-4, Aβ-5, Aβ-6 and Aβ-7), and within-subject factors as 8 electrode sites (FrA1, FrA2, PtA1, PtA2, TeA1, TeA2, V1 and V2). Greenhouse–Geisser-corrected p values were reported. Novel object recognition results were analyzed using ANOVA. Post-hoc comparisons were analyzed with Bonferroni test. Novel object recognition results, delta coherence values, and $A\beta_{1\text{-}42}$ levels were analyzed using ANOVA. Post-hoc comparisons were analyzed using the Bonferroni test. The differences in immunohistochemical staining were analyzed using Kruskal–Wallis one-way ANOVA on ranks, and all pairwise multiple comparisons were performed using the Mann-Whitney U test. Pearson's correlation and linear regression analyses were performed using SPSS to obtain correlation values between $A\beta_{1\text{-}42}$ levels and global-delta and gamma power. Results are expressed as mean ± standard deviation (SD). Significance levels were set at $p<0.05$. All experimenters were blinded to animal experimental group membership during data collection and analyses.

Results

No changes were observed in the general appearance and behavior of animals during the experiment. Body weights of animals were recorded weekly during the experiment and no statistically significant differences were found within and among the groups (Data not shown).

Novel object recognition memory

To avoid bias toward one object, we chose objects made of the same materials with simple shapes and similar sizes. During the initial exposure to the novel object, there were no significant differences among groups in the total time spent in the exploration of both objects (Figure 2A). One hour later, rats were tested for the discrimination between familiar and novel objects. The recognition index values for all groups are presented in Figure 2B. In the test phase, significant differences were found when the novel object exploration was compared between groups [$F(7.56) = 9.28$, $p<0.001$]. Post hoc analysis revealed a significantly lower recognition index in all $A\beta_{1-42}$ injected groups compared with the sham group ($p<0.05$).

Spontaneous EEG power spectrum

The only change observed was in delta and gamma powers, but not in alpha, beta, or theta powers using the repeated measures of ANOVA for the group and/or electrode location in spontaneous EEG. In the present study, we particularly focused on delta and gamma rhythms because significant changes were observed in these frequency bands between the groups. Representative EEG traces, global-delta, and gamma power spectrums are given in Figures 3A, 3B and 3C, respectively. Statistical analyses of EEG recordings revealed that group x location interaction was not significant for delta and gamma rhythms, and hence we evaluated the difference between the groups as global power values, the means of spectral power at the 8 recording electrodes, for these frequency bands.

Spontaneous EEG delta power

In the current study, there was a significant difference between the groups in terms of delta power spectrum [F7.56 = 22.46, p<0.001]. However, rANOVA results for group x location showed no significant interaction effect, indicating that delta power differed between the groups regardless of the electrode locations. Global spectral power values of delta frequency (mean ± SD) in the sham and $A\beta_{1\text{-}42}$-injected groups are given in Figure 3D. In the post hoc comparisons, it was found that the Aβ-4, 5, 6, and 7 groups had higher values for the global delta power spectrum compared with the sham and Aβ-1, 2, 3 groups' overall electrode locations (p<0.001 for all comparisons).

Spontaneous EEG gamma power

There was a significant difference between the groups in terms of gamma power spectrum [F(7.56) = 29.21, p<0.001]. However, rANOVA results for group x location showed no significant interaction effect, which indicated that gamma power differed between the groups regardless of the electrode locations. Global power spectrum values of gamma frequency (mean ± SD) in the sham and $A\beta_{1\text{-}42}$-injected groups are given in Figure 3E. In the post hoc comparisons, it was found that all Aβ groups had lower values for the gamma power spectrum compared with the sham groups' overall electrode locations (p<0.001 for all comparisons).

Spontaneous EEG delta coherence

In the analysis of inter-hemispheric coherence differences, significant changes were only detected in delta coherence between the groups. ANOVA on the delta coherence revealed a significant effect between the groups for FrA1- FrA2 [F(7.56) = 6.92, p<0.001], TeA1-TeA2 [F(7.56) = 4.74, p<0.001] and V1- V2 [F(7.56) = 9.82, p<0.001] electrode pairs.

However, ANOVA revealed no significant group effect on delta coherence for the PtA1-PtA2 electrode pair [$F(7.56) = 0.84$, $p>0.05$]. Delta coherence values for all electrode pairs (mean ± SD) in the sham and $A\beta_{1-42}$-injected groups are given in Table 1. In the post hoc comparisons, it was found that Aβ-4, 5, 6, and 7 groups had lower delta coherence values versus the sham group for the FrA1- FrA2 electrode pair ($p<0.05$ for all comparisons). Furthermore, Aβ-5, 6, and 7 groups had lower delta coherence values compared with the sham group for the TeA1-TeA2 electrode pair ($p<0.01$ for all comparisons). For the V1-V2 electrode pair, significantly lower delta coherence values were found for all $A\beta_{1-42}$-injected groups compared with the sham group ($p<0.001$ for all comparisons). In the analysis of intra-hemispheric coherence differences, ANOVA on delta coherence revealed no significant effect between the groups.

$A\beta_{1-42}$ peptide levels

When we evaluated the $A\beta_{1-42}$ peptide levels in the brain, we observed no difference between the brain regions in intergroup comparisons. ANOVA for $A\beta_{1-42}$ peptide levels revealed a significant treatment effect [$F(7.48) = 136.01$, $p<0.001$]. Values of $A\beta_{1-42}$ peptide levels in the rat brain (mean ± SD) in the sham and experimental groups are given in Figure 4A. Post-hoc comparison tests indicated that $A\beta_{1-42}$ peptide levels were significantly increased in all $A\beta_{1-42}$-injected groups versus the sham group, and significantly increased in a dose-dependent manner from the Aβ-1 group till Aβ-4 group ($p<0.01$ for all comparisons). There was no significant difference between Aβ-4, Aβ-5, 6, and 7 groups ($p>0.05$ for all comparisons).

Correlations between $A\beta_{1-42}$ peptide levels and brain oscillations

Significant correlations were found between changes of brain oscillations and $A\beta_{1-42}$ peptide levels (Figure 4B and 4C) measured in the brain. There were positive correlations between global delta power and $A\beta_{1-42}$ peptide levels ($r= 0.738$, $p<0.001$). In contrast, it was

found that global gamma power and $A\beta_{1-42}$ peptide levels in the brain were negative ($r = -0.758$, $p<0.001$).

Aβ immunohistochemistry

We examined Aβ accumulation in the neocortex regions of the rats to determine the relationship between the electrophysiologic results and AD pathology. The immunohistochemical staining of Aβ in brain regions is shown in Figure 5. As seen in Figure 5B, there is very little intraneuronal Aβ immunolabeling localized in the cortical areas of the sham group. Intense Aβ immunoreactivity was clearly observed in the cytoplasm of neurons in all $A\beta_{1-42}$-injected groups. Quantitative analysis of Aβ-stained sections is presented in Table 2. Statistical analyses revealed that there were significant differences between the groups in all brain regions [FrA1: $H(7) = 18.46$; FrA2: $H(7) = 21.97$; PtA1: $H(7) = 28.41$; PtA2: $H(7) = 21.83$; TeA1: $H(7) = 29.43$; TeA2: $H(7) = 20.41$; V1: $H(7) = 27.75$; V2: $H(7) = 22.14$, $p<0.05$]. In the post hoc comparisons, it was found that all Aβ groups had significantly higher Aβ staining compared with the sham group in all regions ($p<0.05$ for all comparisons). Furthermore, Aβ-2, 3, 4, 5, 6, 7 groups had higher staining compared with the sham and Aβ-1 groups in all brain regions ($p<0.05$ for all comparisons). However, no significant differences in accumulation of Aβ were observed among brain regions for the sham and experimental groups.

Discussion

In the present study, we used a rat AD model based on intracerebroventricular (i.c.v.) injections of aggregated $A\beta_{1-42}$ peptide into the animal brain to investigate possible alterations in brain oscillations and cognitive functions according to the accumulation of $A\beta_{1-42}$ peptide. We observed that i.c.v. application of $A\beta_{1-42}$ peptide led to AD-like memory deficits and EEG changes in the rats. However, the changes in memory impairments were not linear with the concentration of injected $A\beta_{1-42}$ peptide. Consistent with these reports (Wilcock & Esiri, 1982; Arriagada *et al.*, 1992; Berg *et al.*, 1993), our study also shows that evaluating cognitive functions is not sufficient or sensitive enough to determine the localization and relative amount of $A\beta_{1-42}$ peptide accumulated in the brain. Therefore, it is necessary to assess rhythmic electrical oscillations in order to determine early stages of AD depending on the amount of $A\beta_{1-42}$ peptide, as well as cognitive functions. In this study, we particularly focused on delta and gamma rhythms because significant changes were observed in these frequency bands between the groups.

Previous studies reported that characteristic changes in EEG rhythms occurred in patients with AD (Jelic *et al.*, 1996; Huang *et al.*, 2000; Jackson & Snyder, 2008; Yener & Basar, 2010). These changes might provide promising markers for the determination of disease stage. There is a general agreement that EEG is characterized by an increment at low-frequency components (generally in delta and theta rhythms) and a decrement at high-frequency components in patients with AD (alpha, beta, and gamma rhythms) (Jelic *et al.*, 1996; Huang *et al.*, 2000). When the power spectra of spontaneous EEG recorded from patients with AD were assessed, the activity in the delta and theta rhythms were increased, whereas activity in the alpha rhythm was decreased, especially in temporoparietal regions (Jackson & Snyder, 2008; Yener & Basar, 2010). The functional interaction between neural activities in several areas of the brain underlies higher brain functions such as memory and

executive processing (Uhlhaas & Singer, 2006; Sirota *et al.*, 2008). In this context, the cognitive impairment in AD is thought to be due to deteriorated neuronal functional connectivity between several areas of the brain (Uhlhaas & Singer, 2006). Thus, the observed alterations in the activity of delta and gamma rhythms might be indicators of changes in the functional state of the brain. On the other hand, we found no regional differences in delta and gamma rhythms. We also detected no significant differences in Aβ immunostaining between different brain regions in the histologic examinations. This finding partially explains why we observed no significant changes in the electrophysiologic data among different brain regions in all Aβ groups. These findings are in accordance with the results of Stern et al. because they showed experimentally that Aβ plaques might have major effects on the cortical network as a whole due to disrupted cortical synaptic integration (Stern *et al.*, 2004). A possible explanation for these results, the pathologic effect of Aβ peptide on neurons, such as the deterioration of the integrity of neurons and disrupted cortical synaptic integration in a neural network may cause a global change on the whole cortical network due to dense synaptic connection losses.

In the analysis result of total brain $A\beta_{1-42}$ burden obtained using ELISA, we detected that the amount of $A\beta_{1-42}$ peptide in brain regions did not change between the Aβ-injected groups after a certain concentration, despite the administration of Aβ at different concentrations. This result shows that Aβ aggregation in the brain may take place as a result of saturation of the uptake pathway after a certain concentration (4 μg/μL x 5 μL per ventricle). This finding may be a reference for other studies regarding the ideal Aβ concentration to be used in non-transgenic animal models of AD that will be generated through exogenous injection of Aβ because there was intensive Aβ accumulation in the several brain regions and both cognitive and electrophysiologic changes in rats at 4 μg/μL x 5 μL per ventricle. In addition, interestingly, we observed that Aβ accumulated at the surface

and intracellular domains of neurons in all Aβ groups compared with the sham group when Aβ peptide was applied exogenously into the rat cerebral ventricle. A possible explanation for this finding, in view of other studies in the literature, is that exposure of NMDA receptors to Aβ promotes endocytosis of the receptor, thus NMDA receptors may have a potent effect on Aβ uptake (Bi *et al.*, 2002).

We demonstrated for the first time that the Aβ peptide has dose-dependent effects, particularly on delta activity. There were significant changes in delta activity at 4 μg/μL and higher concentrations, but no change was observed at concentrations lower than 4 μg/μL. This increment observed in delta power is consistent with the results of human studies in the literature (Wada *et al.*, 1997; Huang *et al.*, 2000; Shen, 2004; Daulatzai, 2010; Babiloni *et al.*, 2013). Increased delta activity was also reported in diseases, which was associated with white and/or gray matter damage. In normal conditions, abnormal delta activity is considered as a marker of brain damage, namely of deterioration of the subcortical-cortical and/or cortico-cortical connection in awake subjects (Gloor *et al.*, 1977; D'Amelio & Rossini, 2012). Our results suggest that the alterations in delta band activity provide information only about major pathologic changes of the brain seen at advanced stage AD, but not early stages, where the accumulation of $A\beta_{1\text{-}42}$ is lower. Therefore, it is possible to say that delta activity cannot be used as a biomarker for early detection of AD.

On the other hand, we detected that functional brain connectivity was impaired after application of $A\beta_{1\text{-}42}$ only at 4 μg/μL and higher concentrations. With respect to frontal and temporal electrode pairs, it was observed that there was a significant reduction of delta coherence related to $A\beta_{1\text{-}42}$. On the other hand, according to our results, it could be said that functional connectivity between occipital regions is more sensitive to the amount of Aβ peptide because we observed that there was a massive reduction in coherence values between the occipital regions in all Aβ groups compared with the sham group. However, delta

coherence for the parietal electrode pair was not affected by injection of $A\beta_{1-42}$. As a possible explanation for this finding, coherence appears as a consequence of the synchronous activity of different neural networks in the brain. If $A\beta_{1-42}$ peptide injections result in a homogeneous pathology in the parietal region, no significant difference in coherence degrees may be observed. Thus, no change in coherence values may be observed in between the parietal brain regions after i.c.v. injections of $A\beta_{1-42}$.

Earlier studies indicated that gamma oscillations have been observed in the neocortex, amygdala, hippocampus, entorhinal cortex, and striatum as well as other areas (Chrobak & Buzsaki, 1998; Mann *et al.*, 2005; Sirota *et al.*, 2008; Popescu *et al.*, 2009). The common points of these brain regions are the presence of inhibitory interneurons, which show their actions through $GABA_A$ receptors. Synchronization of neurons is substantially more effective by perisomatic inhibitory postsynaptic potentials than dendritic excitatory postsynaptic potentials (Lytton & Sejnowski, 1991). From these findings, it could be said that $GABA_A$ receptor-mediated inhibition is the key component of gamma oscillations. The other key component is the presence of excitatory-inhibitory (E/I) synaptic connections in the brain because weakening of the E/I connection reduces the amplitude of gamma oscillations (Fuchs *et al.*, 2007). These oscillations emerge from the synchronized firing of interconnected excitatory glutamatergic and inhibitory GABAergic interneurons, and its power is modulated by the E/I balance at distinct synaptic sites in the circuit and the intrinsic excitable properties of the neurons. Neurons in the networks interact with each other through their synaptic connections and thereby gamma oscillations typically emerge from the synchronization of E/I interactions (Belluscio *et al.*, 2012; Buzsaki & Wang, 2012). Gamma oscillations have an essential role in higher brain functions such as cognition, attention, and memory (Singer, 1993), and are known to be significantly deteriorated in patients with AD. In agreement with our results, the reduction in the high-frequency content of EEG, which is called EEG slowing,

has been observed in other AD animal models and in vitro studies using Aβ peptide (Pena-Ortega *et al.*, 2012). Furthermore, a significant correlation between the reduction of high-frequency band power and cognitive impairment has also been reported (Jeong, 2004). Besides these findings, researchers showed that interneurons rather than excitatory neurons were affected earlier (around 3-4 months) in experimental AD models (Baglietto-Vargas *et al.*, 2010; Verret *et al.*, 2012). In addition, various neurotransmitter systems that are mediated by glutamate, acetylcholine, serotonin, and dopamine modulate neuronal network activity. Aβ peptide is a neurotoxic agent that disturbs the activity of these systems by acting on neuronal membranes (Klein *et al.*, 2004). On the other hand, Aβ aggregates have been reported to be responsible for cognitive impairment in AD (Mucke *et al.*, 2000; Walsh & Selkoe, 2007). As reported previously, accumulation of Aβ peptide could induce abnormal neuronal oscillations and lead to synaptic failure (Small *et al.*, 2001; Palop & Mucke, 2010; Ma & Klann, 2012). A recent study also demonstrated that Aβ peptide degrades neuronal gamma oscillations, probably through a synaptic dysfunction mechanism (Kurudenkandy *et al.*, 2014). In agreement with this, we found that the power of gamma activity was significantly decreased in all Aβ groups compared with the sham group. Thus, this finding strongly suggests that gamma oscillations might be used as an important biomarker to elicit global alterations caused by the Aβ peptide at initial stages of AD.

In summary, the results of this present study evidence that delta activity is altered only after a significant accumulation of Aβ peptide. From our data, it can be concluded that less than 20 µg in 5 µL $A\beta_{1-42}$ peptide per ventricle (Aβ-4) cannot induce significant alterations in delta activity, whereas all concentrations of $A\beta_{1-42}$ peptide used in this study have effects characterized by a reduction in the gamma activity. Thus, alterations in gamma activity could provide useful information about the initial stages of AD, and may offer a diagnostic biomarker for the early detection of AD.

The limitation of our study was that the injection of Aβ peptide caused peptide accumulation in all brain regions; no differences were observed in the amount of Aβ peptide between the brain regions. The fact that peptide accumulations occurred in all brain regions led to brain oscillations being affected globally. We think that this explains why no regional differences were observed in brain oscillations between the groups. In future studies, by providing Aβ peptide accumulation in a certain brain region, it may be more informative to investigate whether regional differences in brain oscillations can be observed depending of accumulation of Aβ peptide.

Conflict of Interest

The authors declare no conflict of interest.

Acknowledgments

This work was supported by the Scientific and Technological Research Council of Turkey (TUBITAK) (SBAG 315S054).

Abbreviations

AD, Alzheimer's disease; Aβ, amyloid-β; ANOVA, analysis of variance; EEG, electroencephalography; E/I, excitatory-inhibitory; FDG, fluorodeoxyglucose; FFT, Fast Fourier Transform; i.c.v., intracerebroventricular; i.p., intraperitoneal; MRI, magnetic resonance imaging; PET, positron emission tomography, RI, recognition index

Author Contributions

The first author, Enis Hidisoglu, contributed to all aspects of the study (i.e., conception and design; data collection, analysis, and interpretation; drafting and critical revision of the manuscript). The second author, Deniz Kantar-Gok, contributed substantially to the statistical analysis and interpretation of the data. The third author, Hakan Er, contributed to immunohistochemical investigations. The fourth author, Alev Duygu Acun, contributed to experimental design and data collection. The principal investigator, Piraye Yargicoglu, Ph.D., contributed substantially to the conception and design of the study, data interpretation, and drafting and critical revision of the manuscript. All authors give their approval of the final version to be published.

Data accessibility

All data associated with this work is available upon request. Please send your request to the corresponding author (pakkiraz@akdeniz.edu.tr)

References

Albert, M.S., DeKosky, S.T., Dickson, D., Dubois, B., Feldman, H.H., Fox, N.C., Gamst, A., Holtzman, D.M., Jagust, W.J., Petersen, R.C., Snyder, P.J., Carrillo, M.C., Thies, B. & Phelps, C.H. (2011) The diagnosis of mild cognitive impairment due to Alzheimer's disease: Recommendations from the National Institute on Aging-Alzheimer's Association workgroups on diagnostic guidelines for Alzheimer's disease. *Alzheimers Dement*, **7**, 270-279.

Arriagada, P.V., Growdon, J.H., Hedleywhyte, E.T. & Hyman, B.T. (1992) Neurofibrillary Tangles but Not Senile Plaques Parallel Duration and Severity of Alzheimers-Disease. *Neurology*, **42**, 631-639.

Babiloni, C., Carducci, F., Lizio, R., Vecchio, F., Baglieri, A., Bernardini, S., Cavedo, E., Bozzao, A., Buttinelli, C., Esposito, F., Giubilei, F., Guizzaro, A., Marino, S., Montella, P., Quattrocchi, C.C., Redolfi, A., Soricelli, A., Tedeschi, G., Ferri, R., Rossi-Fedele, G., Ursini, F., Scrascia, F., Vernieri, F., Pedersen, T.J., Hardemark, H.G., Rossini, P.M. & Frisoni, G.B. (2013) Resting state cortical electroencephalographic rhythms are related to gray matter volume in subjects with mild cognitive impairment and Alzheimer's disease. *Hum Brain Mapp*, **34**, 1427-1446.

Babiloni, C., Cassetta, E., Binetti, G., Tombini, M., Del Percio, C., Ferreri, F., Ferri, R., Frisoni, G., Lanuzza, B., Nobili, F., Parisi, L., Rodriguez, G., Frigerio, L., Gurzi, M., Prestia, A., Vernieri, F., Eusebi, F. & Rossini, P.M. (2007) Resting EEG sources correlate with attentional span in mild cognitive impairment and Alzheimer's disease. *Eur J Neurosci*, **25**, 3742-3757.

Baglietto-Vargas, D., Moreno-Gonzalez, I., Sanchez-Varo, R., Jimenez, S., Trujillo-Estrada, L., Sanchez-Mejias, E., Torres, M., Romero-Acebal, M., Ruano, D., Vizuete, M., Vitorica, J. & Gutierrez, A. (2010) Calretinin Interneurons are Early Targets of Extracellular Amyloid-beta Pathology in PS1/A beta PP Alzheimer Mice Hippocampus. *J Alzheimers Dis*, **21**, 119-132.

Balducci, C. & Forloni, G. (2011) APP Transgenic Mice: Their Use and Limitations. *Neuromol Med*, **13**, 117-137.

Belluscio, M.A., Mizuseki, K., Schmidt, R., Kempter, R. & Buzsaki, G. (2012) Cross-Frequency Phase-Phase Coupling between Theta and Gamma Oscillations in the Hippocampus. *J Neurosci*, **32**, 423-435.

Bendat, J.S. (1982) Citation Classic - Random Data - Analysis and Measurement Procedures. *Cc/Eng Tech Appl Sci*, 16-16.

Benilova, I., Karran, E. & De Strooper, B. (2012) The toxic Abeta oligomer and Alzheimer's disease: an emperor in need of clothes. *Nature neuroscience*, **15**, 349-357.

Berg, L., Mckeel, D.W., Miller, J.P., Baty, J. & Morris, J.C. (1993) Neuropathological Indexes of Alzheimers-Disease in Demented and Nondemented Persons Aged 80 Years and Older. *Arch Neurol-Chicago*, **50**, 349-358.

Bi, X., Gall, C.M., Zhou, J. & Lynch, G. (2002) Uptake and pathogenic effects of amyloid beta peptide 1-42 are enhanced by integrin antagonists and blocked by NMDA receptor antagonists. *Neuroscience*, **112**, 827-840.

Bickford, R.G. (1976) New Trends in Clinical Electroencephalography. *Practitioner*, **217**, 100-107.

Braidy, N., Munoz, P., Palacios, A.G., Castellano-Gonzalez, G., Inestrosa, N.C., Chung, R.S., Sachdev, P. & Guillemin, G.J. (2012) Recent rodent models for Alzheimer's disease: clinical implications and basic research. *J Neural Transm*, **119**, 173-195.

Buzsaki, G. & Wang, X.J. (2012) Mechanisms of Gamma Oscillations. *Annual Review of Neuroscience, Vol 35*, **35**, 203-225.

Chrobak, J.J. & Buzsaki, G. (1998) Gamma oscillations in the entorhinal cortex of the freely behaving rat. *J Neurosci*, **18**, 388-398.

Corbett, A. & Ballard, C. (2012) New and emerging treatments for Alzheimer's disease. *Expert Opin Emerg Drugs*, **17**, 147-156.

D'Amelio, M. & Rossini, P.M. (2012) Brain excitability and connectivity of neuronal assemblies in Alzheimer's disease: From animal models to human findings. *Prog Neurobiol*, **99**, 42-60.

Daulatzai, M.A. (2010) Conversion of Elderly to Alzheimer's Dementia: Role of Confluence of Hypothermia and Senescent Stigmata - the Plausible Pathway. *J Alzheimers Dis*, **21**, 1039-1063.

Dubois, B., Feldman, H.H., Jacova, C., Dekosky, S.T., Barberger-Gateau, P., Cummings, J., Delocourte, A., Galasko, D., Gauthier, S., Jicha, G., Meguro, K., O'Brien, J., Pasquier, F., Robert, P., Rossor, M., Solloway, S., Stern, Y., Visser, P.J. & Scheltens, P. (2007) Research criteria for the diagnosis of Alzheimer"s disease: revising the NINCDS-ADRDA criteria. *Lancet Neurol*, **6**, 734-746.

Fuchs, E.C., Zivkovic, A.R., Cunningham, M.O., Middleton, S., LeBeau, F.E.N., Bannerman, D.M., Rozov, A., Whittington, M.A., Traub, R.D., Rawlins, J.N.P. & Monyer, H. (2007) Recruitment of parvalbumin-positive interneurons determines hippocampal function and associated behavior. *Neuron*, **53**, 591-604.

Gloor, P., Ball, G. & Schaul, N. (1977) Brain Lesions That Produce Delta Waves in Eeg. *Neurology*, **27**, 326-333.

Gong, L., Li, S.L., Li, H. & Zhang, L. (2011) Ginsenoside Rg1 protects primary cultured rat hippocampal neurons from cell apoptosis induced by beta beta-amyloid protein. *Pharm Biol*, **49**, 501-507.

Huang, C., Wahlund, L.O., Dierks, T., Julin, P., Winblad, B. & Jelic, V. (2000) Discrimination of Alzheimer's disease and mild cognitive impairment by equivalent

EEG sources: a cross-sectional and longitudinal study. *Clin Neurophysiol*, **111**, 1961-1967.

Jack, C.R., Bernstein, M.A., Borowski, B.J., Gunter, J.L., Fox, N.C., Thompson, P.M., Schuff, N., Krueger, G., Killiany, R.J., DeCarli, C.S., Dale, A.M., Carmichael, O.W., Tosun, D., Weiner, M.W. & Initi, A.s.D.N. (2010) Update on the Magnetic Resonance Imaging core of the Alzheimer's Disease Neuroimaging Initiative. *Alzheimers Dement*, **6**, 212-220.

Jackson, C.E. & Snyder, P.J. (2008) Electroencephalography and event-related potentials as biomarkers of mild cognitive impairment and mild Alzheimer's disease. *Alzheimers Dement*, **4**, S137-S143.

Jarrett, J.T., Berger, E.P. & Lansbury, P.T. (1993) The Carboxy Terminus of the Beta-Amyloid Protein Is Critical for the Seeding of Amyloid Formation - Implications for the Pathogenesis of Alzheimers-Disease. *Biochemistry*, **32**, 4693-4697.

Jelic, V., Shigeta, M., Julin, P., Almkvist, O., Winblad, B. & Wahlund, L.O. (1996) Quantitative electroencephalography power and coherence in Alzheimer's disease and mild cognitive impairment. *Dementia*, **7**, 314-323.

Jeong, J.S. (2004) EEG dynamics in patients with Alzheimer's disease. *Clin Neurophysiol*, **115**, 1490-1505.

Klein, W.L., Stine, W.B. & Teplow, D.B. (2004) Small assemblies of unmodified amyloid beta-protein are the proximate neurotoxin in Alzheimer's disease. *Neurobiol Aging*, **25**, 569-580.

Kurudenkandy, F.R., Zilberter, M., Biverstal, H., Presto, J., Honcharenko, D., Stromberg, R., Johansson, J., Winblad, B. & Fisahn, A. (2014) Amyloid-beta-Induced Action Potential Desynchronization and Degradation of Hippocampal Gamma Oscillations Is Prevented by Interference with Peptide Conformation Change and Aggregation. *J Neurosci*, **34**, 11416-11425.

Lecanu, L., Greeson, J. & Papadopoulos, V. (2006) Beta-amyloid and oxidative stress jointly induce neuronal death, amyloid deposits, gliosis, and memory impairment in the rat brain. *Pharmacology*, **76**, 19-33.

Lecanu, L. & Papadopoulos, V. (2013) Modeling Alzheimer's disease with non-transgenic rat models. *Alzheimers Res Ther*, **5**.

Li, Y.Z., Duffy, K.B., Ottinger, M.A., Ray, B., Bailey, J.A., Holloway, H.W., Tweedie, D., Perry, T., Mattson, M.P., Kapogiannis, D., Sambamurti, K., Lahiri, D.K. & Greig, N.H. (2010) GLP-1 Receptor Stimulation Reduces Amyloid-beta Peptide Accumulation and Cytotoxicity in Cellular and Animal Models of Alzheimer's Disease. *J Alzheimers Dis*, **19**, 1205-1219.

Lytton, W.W. & Sejnowski, T.J. (1991) Simulations of Cortical Pyramidal Neurons Synchronized by Inhibitory Interneurons. *Journal of neurophysiology*, **66**, 1059-1079.

Ma, T. & Klann, E. (2012) Amyloid beta: linking synaptic plasticity failure to memory disruption in Alzheimer's disease. *J Neurochem*, **120 Suppl 1**, 140-148.

Malin, D.H., Crothers, M.K., Lake, J.R., Goyarzu, P., Plotner, R.E., Garcia, S.A., Spell, S.H., Tomsic, B.J., Giordano, T. & Kowall, N.W. (2001) Hippocampal injections of amyloid beta-peptide 1-40 impair subsequent one-trial/day reward learning. *Neurobiol Learn Mem*, **76**, 125-137.

Mann, E.O., Suckling, J.M., Hajos, N., Greenfield, S.A. & Paulsen, O. (2005) Perisomatic feedback inhibition underlies cholinergically induced fast network oscillations in the rat hippocampus in vitro. *Neuron*, **45**, 105-117.

Masliah, E., Mallory, M., Alford, M., DeTeresa, R., Hansen, L.A., McKeel, D.W. & Morris, J.C. (2001) Altered expression of synaptic proteins occurs early during progression of Alzheimer's disease. *Neurology*, **56**, 127-129.

McKhann, G.M., Knopman, D.S., Chertkow, H., Hyman, B.T., Jack, C.R., Kawas, C.H., Klunk, W.E., Koroshetz, W.J., Manly, J.J., Mayeux, R., Mohs, R.C., Morris, J.C., Rossor, M.N., Scheltens, P., Carrillo, M.C., Thies, B., Weintraub, S. & Phelps, C.H. (2011) The diagnosis of dementia due to Alzheimer's disease: Recommendations from the National Institute on Aging-Alzheimer's Association workgroups on diagnostic guidelines for Alzheimer's disease. *Alzheimers Dement*, **7**, 263-269.

Mucke, L., Masliah, E., Yu, G.Q., Mallory, M., Rockenstein, E.M., Tatsuno, G., Hu, K., Kholodenko, D., Johnson-Wood, K. & McConlogue, L. (2000) High-level neuronal expression of A beta(1-42) in wild-type human amyloid protein precursor transgenic mice: Synaptotoxicity without plaque formation. *J Neurosci*, **20**, 4050-4058.

Mugantseva, E.A. & Podolski, I.Y. (2009) Animal model of Alzheimer's disease: characteristics of EEG and memory. *Central European Journal of Biology*, **4**, 507-514.

Palop, J.J. & Mucke, L. (2010) Amyloid-beta-induced neuronal dysfunction in Alzheimer's disease: from synapses toward neural networks. *Nature neuroscience*, **13**, 812-818.

Pena-Ortega, F., Solis-Cisneros, A., Ordaz, B., Balleza-Tapia, H. & Lopez-Guerrero, J.J. (2012) Amyloid Beta 1-42 Inhibits Entorhinal Cortex Activity in the Beta-Gamma Range: Role of GSK-3. *Curr Alzheimer Res*, **9**, 857-863.

Popescu, A.T., Popa, D. & Pare, D. (2009) Coherent gamma oscillations couple the amygdala and striatum during learning. *Nature neuroscience*, **12**, 801-U161.

Sanchez-Alavez, M., Chan, S.L., Mattson, M.P. & Criado, J.R. (2007) Electrophysiological and cerebrovascular effects of the alpha-secretase-derived form of amyloid precursor protein in young and middle-aged rats. *Brain Res*, **1131**, 112-117.

Shen, Z. (2004) Brain cholinesterases: II. The molecular and cellular basis of Alzheimer's disease. *Med Hypotheses*, **63**, 308-321.

Sheng, M., Sabatini, B.L. & Sudhof, T.C. (2012) Synapses and Alzheimer's disease. *Cold Spring Harb Perspect Biol*, **4**.

Singer, W. (1993) Synchronization of Cortical Activity and Its Putative Role in Information-Processing and Learning. *Annu Rev Physiol*, **55**, 349-374.

Sirota, A., Montgomery, S., Fujisawa, S., Isomura, Y., Zugaro, M. & Buzsaki, G. (2008) Entrainment of Neocortical Neurons and Gamma Oscillations by the Hippocampal Theta Rhythm. *Neuron*, **60**, 683-697.

Small, D.H., Mok, S.S. & Bornstein, J.C. (2001) Alzheimer's disease and AP toxicity: from top to bottom. *Nat Rev Neurosci*, **2**, 595-598.

Sperling, R. (2011) The potential of functional MRI as a biomarker in early Alzheimer's disease. *Neurobiol Aging*, **32**, S37-S43.

Stern, E.A., Bacskai, B.J., Hickey, G.A., Attenello, F.J., Lombardo, J.A. & Hyman, B.T. (2004) Cortical synaptic integration in vivo is disrupted by amyloid-beta plaques. *J Neurosci*, **24**, 4535-4540.

Turner, P.R., O'Connor, K., Tate, W.P. & Abraham, W.C. (2003) Roles of amyloid precursor protein and its fragments in regulating neural activity, plasticity and memory. *Prog Neurobiol*, **70**, 1-32.

Uhlhaas, P.J. & Singer, W. (2006) Neural synchrony in brain disorders: relevance for cognitive dysfunctions and pathophysiology. *Neuron*, **52**, 155-168.

Uylings, H.B. & de Brabander, J.M. (2002) Neuronal changes in normal human aging and Alzheimer's disease. *Brain and cognition*, **49**, 268-276.

Verret, L., Mann, E.O., Hang, G.B., Barth, A.M.I., Cobos, I., Ho, K., Devidze, N., Masliah, E., Kreitzer, A.C., Mody, I., Mucke, L. & Palop, J.J. (2012) Inhibitory Interneuron Deficit Links Altered Network Activity and Cognitive Dysfunction in Alzheimer Model. *Cell*, **149**, 708-721.

Wada, Y., Nanbu, Y., Jiang, Z.Y., Koshino, Y., Yamaguchi, N. & Hashimoto, T. (1997) Electroencephalographic abnormalities in patients with presenile dementia of the Alzheimer type: Quantitative analysis at rest and during photic stimulation. *Biol Psychiat*, **41**, 217-225.

Walsh, D.M. & Selkoe, D.J. (2007) A beta Oligomers - a decade of discovery. *J Neurochem*, **101**, 1172-1184.

Wang, J., Ikonen, S., Gurevicius, K., van Groen, T. & Tanila, H. (2002) Alteration of cortical EEG in mice carrying mutated human APP transgene. *Brain Res*, **943**, 181-190.

Wesson, D.W., Nixon, R.A., Levy, E. & Wilson, D.A. (2011) Mechanisms of neural and behavioral dysfunction in Alzheimer's disease. *Mol Neurobiol*, **43**, 163-179.

Wilcock, G.K. & Esiri, M.M. (1982) Plaques, Tangles and Dementia - a Quantitative Study. *J Neurol Sci*, **56**, 343-356.

Yener, G.G. & Basar, E. (2010) Sensory evoked and event related oscillations in Alzheimer's disease: a short review. *Cogn Neurodynamics*, **4**, 263-274.

Zhang, R., Xue, G.Z., Wang, S.D., Zhang, L.H., Shi, C.J. & Xie, X. (2012) Novel Object Recognition as a Facile Behavior Test for Evaluating Drug Effects in A beta PP/PS1 Alzheimer's Disease Mouse Model. *J Alzheimers Dis*, **31**, 801-812.

Table 1. Dose-dependent effects of $A\beta_{1-42}$ peptide on intrahemispheric delta coherence. Results are expressed as mean ± standard deviation (SD). Bold indicates significant difference of groups Aβ-4, 5, 6, and 7 compared with the sham group for the FrA1-FrA2 electrode pair ($p<0.05$), Aβ-5, 6, and 7 groups compared with the sham group for the TeA1-TeA2 electrode pair ($p<0.01$), and all Aβ groups compared with the sham group for the V1-V2 electrode pair ($p < 0.001$).

	FrA1-FrA2	PtA1-PtA2	TeA1-TeA2	V1-V2
Sham	0,79±0,19	0,64±0,15	0,95±0,04	0,65±0,17
Aβ-1	0,70±0,16	0,51±0,17	0,84±0,18	**0,31±0,20**
Aβ-2	0,62±0,25	0,48±0,24	0,87±0,05	**0,41±0,13**
Aβ-3	0,62±0,15	0,27±0,15	0,87±0,03	**0,24±0,16**
Aβ-4	**0,41±0,28**	0,35±0,21	0,83±0,14	**0,28±0,23**
Aβ-5	**0,49±0,07**	0,35±0,34	**0,64±0,30**	**0,29±0,14**
Aβ-6	**0,40±0,19**	0,38±0,23	**0,64±0,24**	**0,23±0,07**
Aβ-7	**0,44±0,15**	0,47±0,20	**0,62±0,13**	**0,20±0,15**

Table 2. The result of quantitative analysis of Aβ-stained sections. Results are expressed as mean ± standard deviation (SD). Bold indicates significant difference of sham group compared with all Aβ groups ($p<0.05$).

	FrA1	FrA2	PtA1	PtA2	TeA1	TeA2	V1	V2
Sham	**6,07±1,32**	**6,11±0,96**	**6,23±0,83**	**7,03±1,24**	**6,46±0,72**	**6,02±0,32**	**6,09±0,82**	**6,30±0,41**
Aβ-1	17,66±1,61	18,31±3,15	17,01±1,31	18,91±1,79	15,44±0,97	16,79±0,67	18,82±0,61	17,30±0,43
Aβ-2	16,54±1,82	15,87±1,45	16,14±0,83	17,51±1,77	17,00±1,45	18,62±0,49	17,56±0,	18,49±0,51
Aβ-3	17,35±2,12	16,39±2,04	16,18±1,23	15,83±0,22	16,28±1,09	14,49±0,76	17,55±1,20	18,54±0,64
Aβ-4	17,33±1,66	18,89±1,21	16,33±1,07	16,52±0,71	18,24±1,75	19,13±0,36	17,45±0,97	18,99±0,49
Aβ-5	17,68±2,19	18,39±3,43	18,41±1,06	19,22±0,81	18,05±0,99	19,24±0,23	16,55±1,10	17,59±0,67
Aβ-6	17,12±2,49	19,23±2,04	16,61±1,45	17,85±0,44	15,95±1,54	17,74±0,69	15,92±1,57	16,26±0,69
Aβ-7	19,84±1,28	17,25±0,47	15,81±1,37	19,90±0,26	16,87±0,86	17,40±0,57	17,21±1,03	19,58±0,52

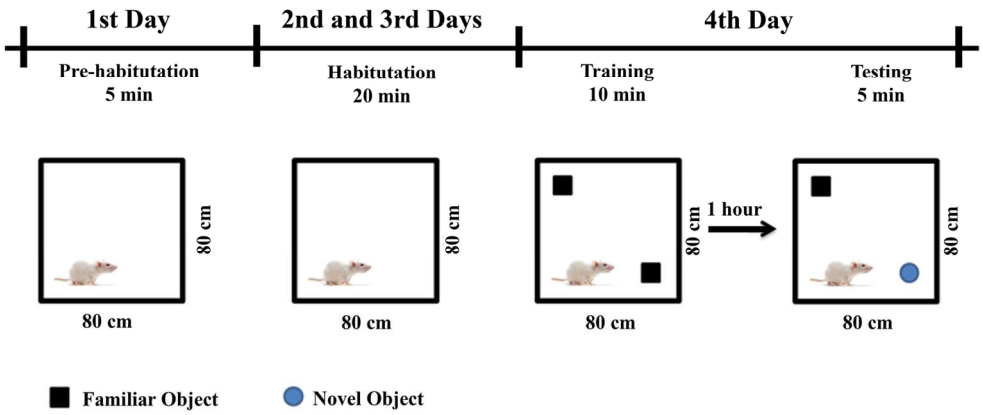

Figure 1. Schematic representation of novel object recognition test. Following pre-habituation and habituation sessions in the empty box, the rats were allowed to explore an identical pair of objects placed in the boxes for 10 min, and then returned to their home cages. One hour later, animals were placed back in the same box in which one of the two familiar objects was switched for a novel object. The time the rats spent exploring the two objects was recorded.

69x30mm (600 x 600 DPI)

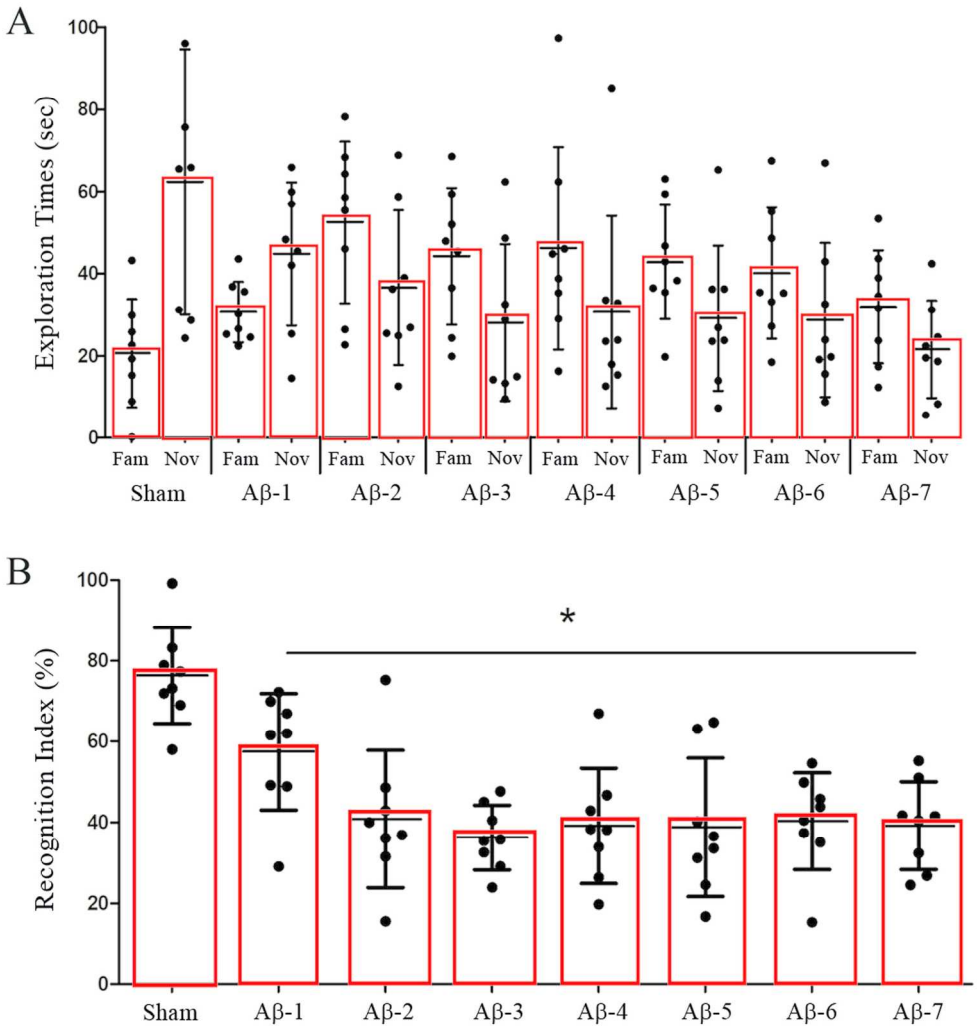

Figure 2. Effects of different doses of Aβ1-42 peptide on learning and memory. (A), The times spent exploring the novel and familiar objects on day 4 of testing are shown. Fam and Nov represent 'familiar' and 'novel' objects, respectively. (B), The graph compares the effects of different concentrations of Aβ1-42 peptide on the recognition index in all groups. Aβ1-42 peptide injection significantly reduced recognition index compared with the sham group (n=10 per group). Results are expressed as mean ± standard deviation. *p < 0.05.

94x99mm (600 x 600 DPI)

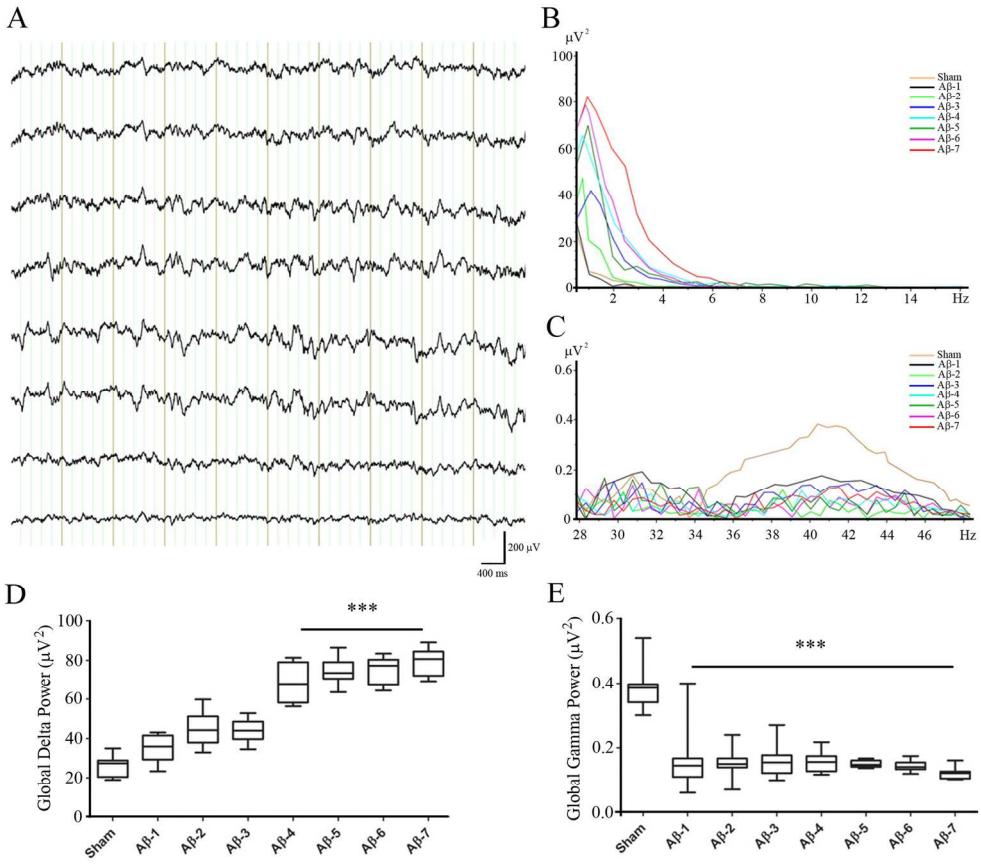

Figure 3. Dose-dependent effects of Aβ1-42 peptide on spontaneous EEG activity. (A), Representative 10-second EEG traces from a rat cortex recorded using multi-electrodes in the sham group. (B) and (C), Power spectrums of global delta- and gamma-band activity in all groups, respectively. (D) and (E), Global spectral powers of delta and gamma frequency for all groups, respectively (n=10 per group). Results are expressed as mean ± standard deviation.
*** p<0.001.

88x77mm (600 x 600 DPI)

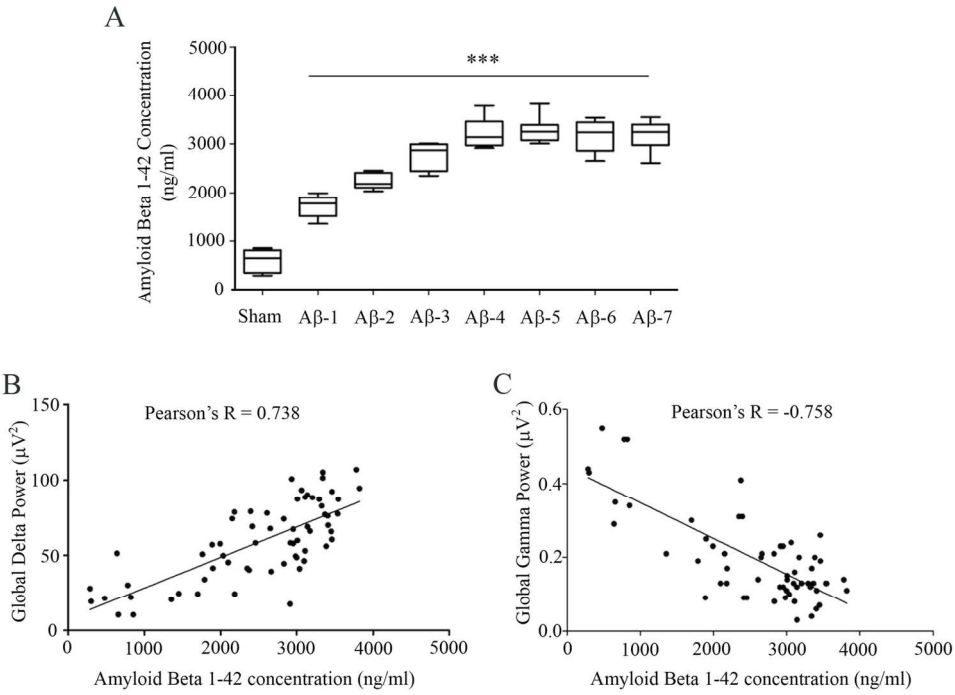

Figure 4. Aβ1-42 peptide levels in the rat brain and degree of correlation between the amount of Aβ1-42 peptide and brain oscillations. (A), Aβ1-42 peptide levels in rat brains obtained using ELISA in all groups (n=7 per group). The Aβ1-42 ELISA results are expressed as mean ± standard deviation. (B) and (C), Correlation degree between Aβ1-42 peptide levels and global-delta and -gamma power, respectively. Significant correlations were found between changes of brain oscillations and Aβ1-42 peptide levels. *** $p<0.001$.

76x53mm (600 x 600 DPI)

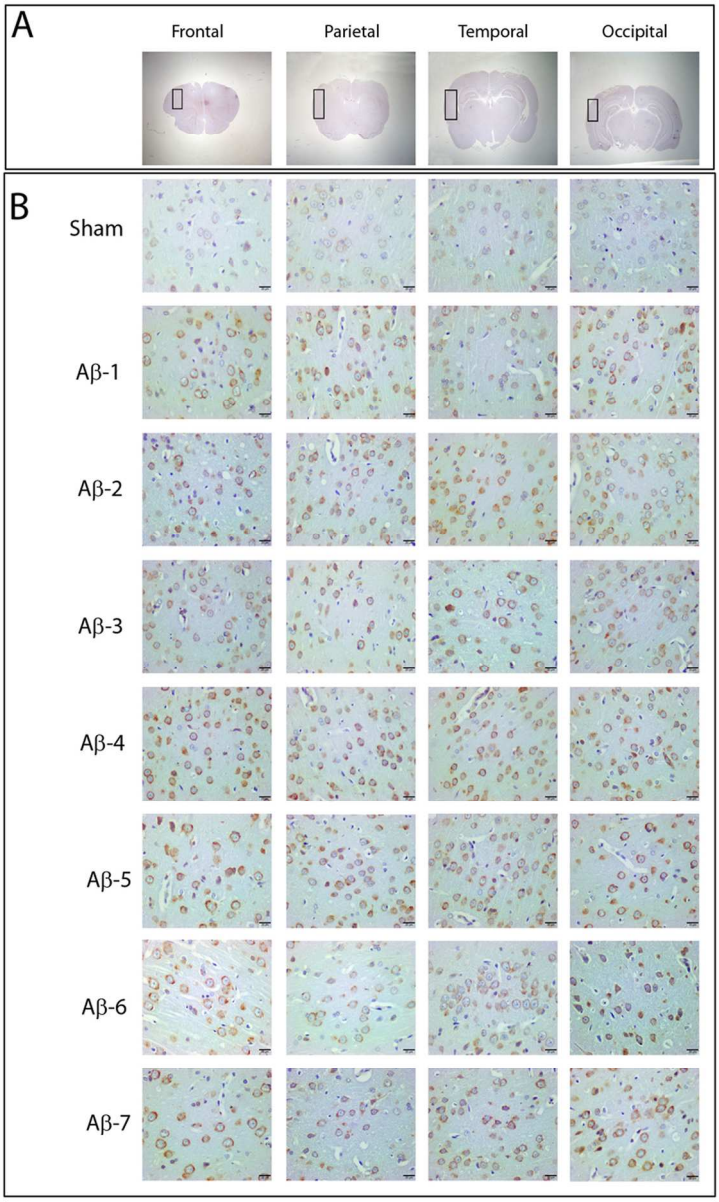

Figure 5. Immunostaining of Aβ1-42 in rat brains from sham and Aβ1-42 peptide injected groups. (A), Representative total brains from frontal, parietal, temporal and occipital regions of the rat brain. Rectangles are the cortex regions from which higher magnification micrographs were taken (x40). (B), Higher magnification (x40) Aβ immunostaining micrographs of brain cortex from the frontal, parietal, temporal, and occipital regions of the sham and Aβ1-42 peptide-injected groups. (All scale bars are 20μm).

199x330mm (600 x 600 DPI)

Graphical Abstract Text

This study focuses on dose dependent effects of Aβ peptide on brain activity in rats. Our findings demonstrate that less than Aβ peptide 20 μg in 5 μL cannot induce alterations in delta activity, whereas Aβ peptide doses, between 5 and 50 μg in 5 μL, have effect characterized by a reduction in gamma activity. Thus, delta activity changes may be thought to represent the major pathological stages of AD, while gamma activity changes may offer as a diagnostic biomarker for initial stages of AD.

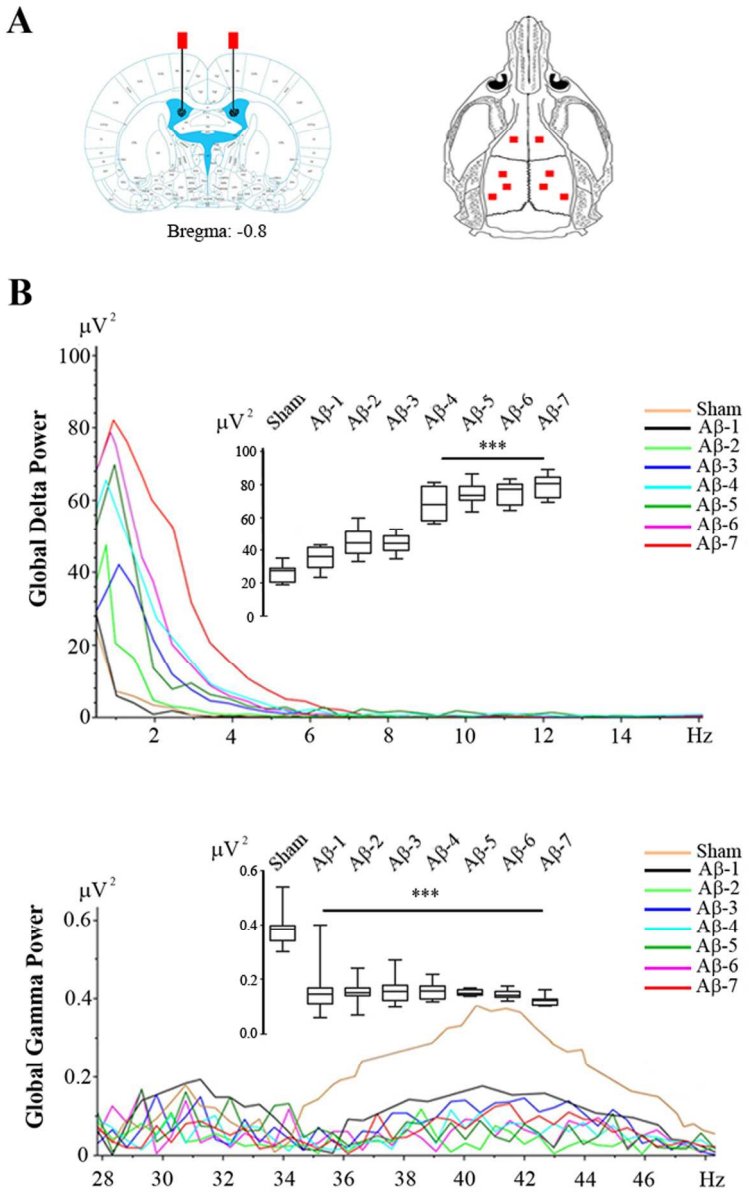

(A), Representative injection sites of 0.9 % NaCl or Aβ 1-42 peptide, and spontaneous EEG acquisition points. (B) Dose dependent effects of Aβ 1-42 peptide on spontaneous EEG activity.